1em 0pt

LME-MPM applied to quasi-brittle fracture.

Miguel Molinos[a1], and Pedro Navas[a2]

[a] *ETSI Caminos, Canales y Puertos, Universidad Politéctnica de Madrid. c. Prof. Aranguren 3, 28040 Madrid, Spain*

Abstract

The objective of this work is to introduce an alternative technique to address the fracture process of brittle and quasi-brittle materials under the material point method (MPM) framework. With this purpose the eigensoftening algorithm, developed originally for the optimal transportation meshfree (OTM) approximation scheme, is extended to the MPM with the aim of present a suitable alternative to the existing fracture algorithms developed for the MPM. The good fitting in the predictions made by the eigensoftening algorithm against both analytical and experimental results proofs the well performance of the method under challenging loads.

Keywords: Quasi brittle fracture, Local-*max-ent* approximation, Material Point Method, Solid Dynamics

1. Introduction

The simulation of fracture propagation in a more accurate and effective way can be considered as one of the original drivers for developing novel spatial discretization methods such as meshfree methods like the material point method (MPM). Presence of cracks are a violation of the continuity requirement of the finite element approach (MPM).

The MPM does not suffer from the above difficulties. Discontinuities can be described in two ways. One is to abandon the single-valued velocity field property near the crack by using two or more background meshes, and the other is to use failed material points to approximately describe the crack.

In the first approach,

[1]Corresponding author: m.molinos@outlook.es

[2]Corresponding author: p.navas@upm.es

2. The meshfree methodology

The popularity of MPM has increase notoriously during the recent years due to its ability to deal with large strain problems without mesh distorsion issues inherent to mesh based methods like FEM, see Zdzislaw [1]. However, in the simulations made with the original MPM, there are numerical noises when particles crossing the cell boundaries.

2.1. The Material Point Method

For the spatial discretization, two sets of points are introduced in the MPM. First, the nodes, this points are considered fixed in the space and are in charge of computing all the kinematic fields such forces f_I, accelerations a_I and velocities v_I. And second the material points or particles. They are in charge of the discretization of the continuum, and store the local state $(\sigma_p, \varepsilon_p)$.

2.2. Spatial discretization : Local-max-ent approximants

Local maximum-entropy (or local *max-ent*) approximation scheme was introduced by Arroyo & Ortiz (2006)[2] as a bridge between finite elements and meshfree methods. The key idea of the shape functions is to interpret the nodal of a shape function N_I as a probability. This allow us to introduce two important limits: the principle of maximum-entropy (*max-ent*) statistical inference stated by [3], and the Delaunay triangulation which ensures the minimal width of the shape function. To reach to a compromise between two competing objectives, a Pareto set is defined as,

$$\text{(LME)}_\beta \text{ For fixed } \vec{x} \text{ minimise } f_\beta(\vec{x}_p, N_I) = \beta U(\vec{x}_p, N_I) - H(N_I)$$

$$\text{subject to } \begin{cases} N_I \geq 0, \text{ I=1, ..., n} \\ \sum_{I=1}^{N_n} N_I = 1 \\ \sum_{I=1}^{N_n} N_I \vec{x}_I = \vec{x} \end{cases}$$

where $H(N_I)$ is the entropy of the system of nodes following the definition given by Shannon (1948) [4], and $U(\vec{x}_p, N_I) = \sum_I N_I |\vec{x}_p - \vec{x}_I|^2$ a magnitude of the shape function width. The regularization o *thermalization* parameter between the two criterion β has Pareto optimal values in the range $(0, \infty)$. The unique solution of the local max-ent problem $(\text{LME})_\beta$ is:

$$N_I^*(\vec{x}) = \frac{\exp\left[-\beta\ |\vec{x} - \vec{x}_I|^2 + \vec{\lambda}^* \cdot (\vec{x} - \vec{x}_I)\right]}{Z(\vec{x}, \vec{\lambda}^*(\vec{x}))} \tag{1}$$

where $Z(\vec{x}, \vec{\lambda}^*(\vec{x}))$ is the *partition function* defined as,

$$Z(\vec{x}, \vec{\lambda}) = \sum_{I=1}^{N_n} \exp\left[-\beta \left|\vec{x} - \vec{x}_I\right|^2 + \vec{\lambda} \cdot (\vec{x} - \vec{x}_I)\right] \tag{2}$$

and evaluated in the unique minimiser $\vec{\lambda}^*(\vec{x})$ for the function $\log Z(\vec{x}, \vec{\lambda})$. The traditional way to obtain such a minimiser is using (3) to calculate small increments of $\partial\vec{\lambda}$ in a Newton-Raphson approach. Where $\mathbf{J}$ is the Hessian matrix, defined by:

$$\mathbf{J}(\vec{x}, \vec{\lambda}, \beta) \equiv \frac{\partial \vec{r}}{\partial \vec{\lambda}} \tag{3}$$

$$\vec{r}(\vec{x}, \vec{\lambda}, \beta) \equiv \frac{\partial \log Z(\vec{x}, \vec{\lambda})}{\partial \vec{\lambda}} = \sum_{I}^{N_n} p_I(\vec{x}, \vec{\lambda}, \beta)\,(\vec{x} - \vec{x}_I) \tag{4}$$

In order to obtain the first derivatives of the shape function ∇N_I^*, can be computed as,

$$\nabla N_I^* = N_I^* \left(\nabla f_I^* - \sum_{J}^{N_n} N_J^* \nabla f_J^*\right) \tag{5}$$

where

$$f_I^*(\vec{x}, \vec{\lambda}, \beta) = -\beta \left|\vec{x} - \vec{x}_I\right|^2 + \vec{\lambda}^* (\vec{x} - \vec{x}_I) \tag{6}$$

Employing the chain rule over (5), rearranging and considering β as a constant, Arroyo and Ortiz [2] obtained the following expression for the gradient of the shape function.

$$\nabla N_I^* = -N_I^* \left(\mathbf{J}^*\right)^{-1} (\vec{x} - \vec{x}_I) \tag{7}$$

The regularization parameter β of LME shape functions may be controlled by adjusting a dimensionless parameter, $\gamma = \beta h^2$ [2], where h is defined as a measure of the nodal spacing. Since N_I is defined in the entire domain, in practice, the shape function decay $\exp(-\beta\vec{r})$ is truncated by a given tolerance, 10^{-6}, for example, would ensure a reasonable range of neighbours, see [2] for details. This tolerance defines the limit values of the influence radius and is used thereafter to find the neighbour nodes of a given integration point.

2.3. Temporal discretization

This research is devoted to capture the challenging process of fracture during high velocity impacts. To capture the presence of elastic shock waves

triggered by the fracture process. Here we adopt a explicit predictor-corrector time integration scheme. It is based in the Newmark a-form $\gamma = 0.5$ and $\beta = 0$ which is the central difference explicit. In a first stage, the nodal velocity predictor is computed following (8),

$$\vec{v}_I^{k+1} = \frac{N_{Ip}^k m_p (\vec{v}_p^k + (1-\gamma)\ \Delta t\ \vec{a}_p^k)}{m_I} \tag{8}$$

This way of computing the nodal predictor is both numerically stable and minimize the computational effort. Once nodal velocity are obtained, the essential boundary conditions are imposed. And in the following, the "classic" MPM algorithm continues to reach to the equilibrium equation (**??**). Here we continue with the *corrector* stage, due to the fact that we already have nodal velocity, this step is computed in the same way as in FEM,

$$\vec{v}_I^{k+1} = \vec{v}_I^{pred} + \gamma\ \Delta t\ \frac{\vec{f}_I^{k+1}}{\mathbf{m}_I^{k+1}} \tag{9}$$

Finally updated particle kinetics are computed using nodal values as,

$$\vec{a}_p^{k+1} = \frac{N_{Ip}^k \vec{f}_I^k}{\mathbf{m}_I^k} \tag{10}$$

$$\vec{v}_p^{k+1} = \vec{v}_p^n + \Delta t\ \frac{N_{Ip}^k\ \vec{f}_I^k}{\mathbf{m}_I^k} \tag{11}$$

$$\vec{x}_p^{k+1} = \vec{x}_p^n + \Delta t\ N_{Ip}^k\ \vec{v}_I^k + \frac{1}{2}\Delta t^2\ \frac{N_{Ip}^k\ \vec{f}_I^k}{\mathbf{m}_I^k} \tag{12}$$

The complete pseudo-algorithm it is summarized in Appendix A.

2.4. Fracture modelling approach

Within the context of MPM formulation, fracture can be modelled by failing particles according to a suitable criterion. When material points are failed, they are assumed to have a null stress tensor. Navas *et al.* (2017)[5] developed a eigensoftening algorithm as an extension for quasi-brittle materials of the eigenerosion proposed by Pandolfi & Ortiz (2012)[6] for fracture of brittle materials. A comparison between both in [5] shows that the eigenerosion algorithm significantly overestimates the tensile stress and the strain peaks, while it captures the forces and crack patterns accurately. On the other hand eigensoftening algorithm agree very well with experimental results in all the aspects. Furthermore, this algorithm has also proof its accuracy for complex fracture patters such the present in fiber reinforces concrete (FRC), [7].

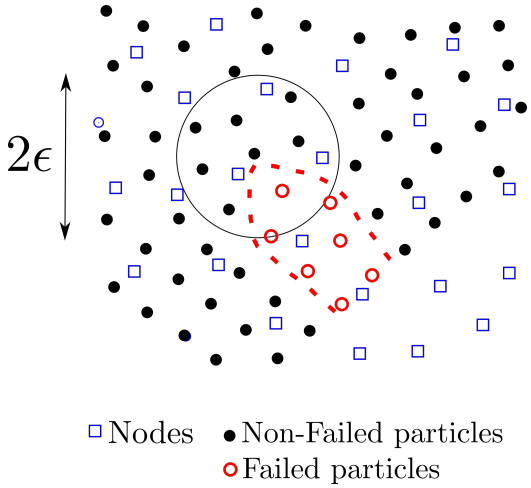

Figure 1: Scheme of a linear cohesive law, where the shaded area is G_f, f_t is the tensile strength, and w_c is the critical opening displacement.

$$G_p^{k+1} = \frac{C_\epsilon}{m_p^{k+1}} \sum_{x_q^{k+1} \in B_\epsilon(x_p^{k+1})} m_q W_q^{k+1} \tag{13}$$

$$m_p^{k+1} = \sum_{x_q^{k+1} \in B_\epsilon(x_p^{k+1})} m_q \tag{14}$$

where $B_\epsilon(x_p^{k+1})$ is the sphere of radius ϵ centered at x_p^{k+1} known as the ϵ-neighborhood of the material point, m_p^{k+1} is the mass of the neighborhood at step $k+1$, W_q^{k+1} is the current free-energy density per unit mass as the material point x_q^{k+1} of the neighborhood, finally C_ϵ is a normalizing constant. This configuration conveniently is sketched in Figure 1. The material point fails when G_p^{k+1} surpasses a critical energy release rate that measures the material-specific energy, G_F. The convergence of this approach has been analyzed by Schmidt *et al.* (2009)[8], who proof that it converges to the Griffith fracture when discretization size tends to zero. It is necessary to point out that when a material point overpass the critical energy, its contribution to the internal forces vector is set to zero, but its contribution to the mass matrix is maintained. The mass of a material point is discarded only when an eroded material point is not connected to any nodes.

As can be noticed, in the eigenerosion algorithm an energetic criterion is adopted. Due to that fact, unrealistic stress concentration (higher than tensile strength) in quasi-brittle materials, see [5]. To overcome this limitation, the aforementioned authors proposed the concept of eigensoftening to

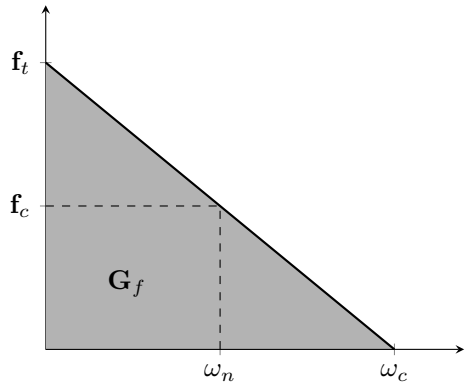

Figure 2: Scheme of a linear cohesive law, where the shaded area is G_f, f_t is the tensile strength, and w_c is the critical opening displacement.

take in to account the gradual failure in quasi-brittle materials. The concept is inspired in the cohesive fracture widely employed in the context of FEM [**?**]. This gradual failure criterion is plotted in figure , where a linear decreasing cohesive law is presented to illustrate the concept here described. In the picture, the shaded area represents the static fracture energy per unit of area, G_F. As we can see, a cohesive crack appears when the maximum tensile strength, f_t is reached. Once the opening displacement w takes the value of the critical crack displacement w_c, a stress-free crack is attained. For intermediate values

$$\delta W_{p,\epsilon} = \frac{\partial G_p}{C_\epsilon} = \frac{1}{m_p} \sum_{x_q^{k+1} \in B_\epsilon(x_p^{k+1})} m_q \sigma_{q,I} \delta\epsilon_q \tag{15}$$

$$\delta W_{p,\epsilon} = \frac{\delta\epsilon_p}{m_p} \sum_{x_q^{k+1} \in B_\epsilon(x_p^{k+1})} m_q \sigma_{q,I} \tag{16}$$

$$\delta\sigma_{p,c} = \frac{1}{m_p} \sum_{x_q^{k+1} \in B_\epsilon(x_p^{k+1})} m_q \sigma_{q,I} \tag{17}$$

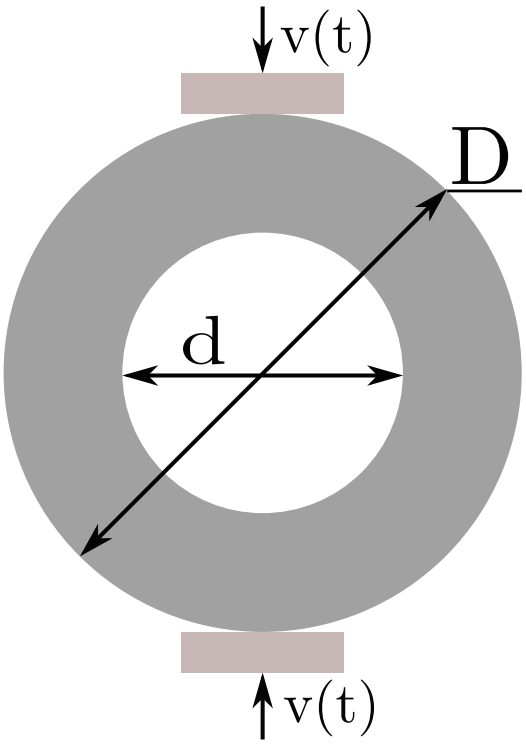

Figure 3: Geometry and boundary condition of the Brazilian test.

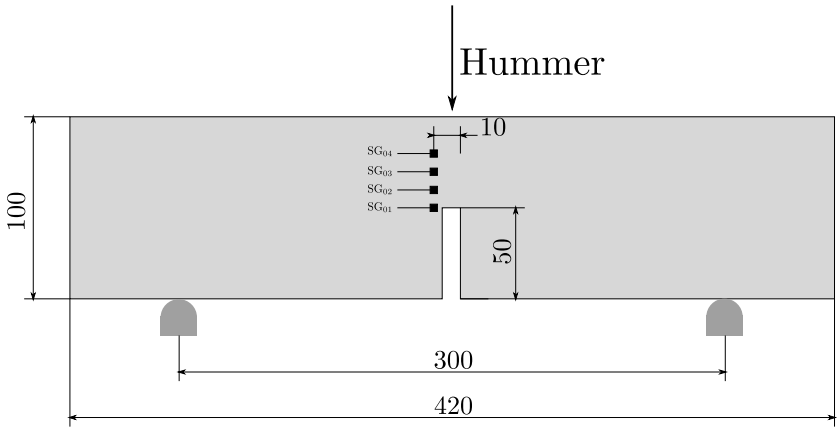

Figure 4: Geometry and boundary condition of the drop-weight impact test.

3. Cases of study and discussion

3.1. Comparison with analytical solution

3.2. Brazilian test

3.3. Drop-weight impact test

4. Conclusions

Acknowledgements

The first author acknowledges the fellowship Agustn de Betancourt 262390106114.

Appendix A. Explicit Predictor-Corrector algorithm

Appendix B. Eigensoftening Algorithm

References

[1] W. Zdzislaw, The material point method in large strain engineering problems, Computer Methods in Applied Mechanics and Engineering 193 (39-41 SPEC. ISS.) (2004) 4417–4438. doi:10.1016/j.cma.2004.01.035.

[2] M. Arroyo, M. Ortiz, Local maximum-entropy approximation schemes: A seamless bridge between finite elements and meshfree methods, International Journal for Numerical Methods in Engineeringdoi:10.1002/nme.1534.

[3] E. Jaynes, Information Theory and Statistical Mechanics, The Physical Review 106 (4) (1957) 620–630.

[4] C. E. Shannon, A Mathematical Theory of Communication, Bell System Technical Journaldoi:10.1002/j.1538-7305.1948.tb01338.x.

[5] P. Navas, R. Yu, B. Li, G. Ruiz, Modeling the dynamic fracture in concrete: an eigensoftening meshfree approach, International Journal of Impact Engineering 113. doi:10.1016/j.ijimpeng.2017.11.004.

[6] A. Pandolfi, M. Ortiz, An eigenerosion approach to brittle fracture., International Journal for Numerical Methods in Engineering 92 (2012) 694–714.

[7] P. Navas, R. Yu, G. Ruiz, Meshfree modeling of the dynamic mixed-mode fracture in frc through an eigensoftening approach, Engineering Structures 172. doi:10.1016/j.engstruct.2018.06.010.

[8] B. Schmidt, F. Fraternali, M. Ortiz, Eigenfracture: an eigendeformation approach to variational fracture., SIAM J. Multiscale Model. Simul. 7 (2009) 1237–1266.

Algorithm Explicit Predictor-Corrector scheme

Update mass matrix:

$$\mathbf{m}_I = N_{Ip}^k \; m_p,$$

Explicit Newmark Predictor:

$$\vec{v}_I^{pred} = \frac{N_{Ip}^k m_p (\vec{v}_p^k + (1-\gamma) \; \Delta t \; \vec{a}_p^k)}{m_I}$$

Impose essential boundary conditions: At the fixed boundary, set $\vec{v}_I^{pred} = 0$. **Deformation tensor increment calculation**.

$$\dot{\varepsilon_p}^{k+1} = \left[\vec{v}_I^{pred} \otimes grad(N_{Ip}^{k+1}) \right]^s$$
$$\Delta\varepsilon_p^{k+1} = \Delta t \; \dot{\varepsilon_p}^{k+1}$$

Update the density field:

$$\rho_p^{k+1} = \frac{\rho_p^k}{1 + tra\left[\Delta\varepsilon_p^{k+1}\right]}.$$

Compute damage parameter: **Balance of forces calculation**: Calculate the total grid nodal force $\vec{f}_I^{k+1} = (1-\chi)\vec{f}_I^{int,k+1} + \vec{f}_I^{ext,k+1}$ evaluating (**??**) and (**??**) in the time step $k+1$. In the grid node I is fixed in one of the spatial dimensions, set it to zero to make the grid nodal acceleration zero in that direction. **Explicit Newmark Corrector**:

$$\vec{v}_I^{k+1} = \vec{v}_I^{pred} + \gamma \; \Delta t \; \frac{\vec{f}_I^{k+1}}{\mathbf{m}_I^{k+1}}$$

Update particles lagrangian quantities:

$$\vec{a}_p^{k+1} = \frac{N_{Ip}^k \vec{f}_I^k}{\mathbf{m}_I^k}$$
$$\vec{v}_p^{k+1} = \vec{v}_p^n + \Delta t \; \frac{N_{Ip}^k \; \vec{f}_I^k}{\mathbf{m}_I^k}$$
$$\vec{x}_p^{k+1} = \vec{x}_p^n + \Delta t \; N_{Ip}^k \; \vec{v}_I^k + \frac{1}{2}\Delta t^2 \; \frac{N_{Ip}^k \; \vec{f}_I^k}{\mathbf{m}_I^k}$$

Reset nodal values

Algorithm 2 Compute damage parameter χ_P^{k+1}

Particle statusNumber of particles: N_p ϵ-neighbourhood of each particle p : $B_{\epsilon,p}$ Material data Tensile strength: $f_{t,p}$ Bandwidth of the cohesive fracture: $h_{\epsilon,p}$ Critical opening displacement: w_c Return damage parameter $\chi := \{\chi_p\}$ $\chi_p \leftarrow \chi_p^k$ p to N_p $\chi_p = 0$ $\epsilon_{f,p} = 0$ $q \in B_{\epsilon,p}$ $\chi_q < 1$ $\sum m_p \sigma_{p,I} \leftarrow \sum m_p \sigma_{p,I} + m_q \sigma_{q,I}$ $m_p \leftarrow m_p + m_q$ $\sigma_{p,\epsilon} \leftarrow \frac{1}{m_p} \sum m_p \sigma_{p,I}$ $\sigma_{p,\epsilon} > f_{t,p}$ $\epsilon_{f,p} = \epsilon_{I,p}$ $[\chi_p \neq 1$ $\epsilon_{f,p} > 0]$ $\chi_p^{k+1} \leftarrow \min\left\{1, \max\{\chi_p^k, \frac{(\epsilon_{I,p} - \epsilon_{f,p})\ h_{\epsilon,p}}{w_c}\}\right\}$